Available online at www.sciencedirect.com
ScienceDirect
Bioorganic & Medicinal Chemistry 15 (2007) 3801–3817
Bioorganic & Medicinal Chemistry

Analysis of the inhibition of mammalian carboxylesterases by novel fluorobenzoins and fluorobenzils

Latorya D. Hicks,[a] Janice L. Hyatt,[a] Teri Moak,[b] Carol C. Edwards,[a] Lyudmila Tsurkan,[a] Monika Wierdl,[a] Antonio M. Ferreira,[c] Randy M. Wadkins[b] and Philip M. Potter[a,*]

[a]*Department of Molecular Pharmacology, St. Jude Children's Research Hospital, Memphis, TN 38105, USA*
[b]*Department of Chemistry and Biochemistry, University of Mississippi, University, MS 38677, USA*
[c]*Hartwell Center for Bioinformatics and Biotechnology, St. Jude Children's Research Hospital, Memphis, TN 38105, USA*

Received 29 January 2007; revised 23 February 2007; accepted 8 March 2007
Available online 12 March 2007

Abstract—We have synthesized and assessed the ability of symmetrical fluorobenzoins and fluorobenzils to inhibit mammalian carboxylesterases (CE). The majority of the latter were excellent inhibitors of CEs however unexpectedly, the fluorobenzoins were very good enzyme inhibitors. Positive correlations were seen with the charge on the hydroxyl carbon atom, the carbonyl oxygen, and the Hammett constants for the derived K_i values with the fluorobenzoins.

1. Introduction

Carboxylesterases (CEs) are ubiquitous enzymes responsible for the detoxification of xenobiotics.[1] It has been reported that CEs can metabolize a wide variety of ester containing compounds including clinical drugs such as, meperidine, flumazenil, procaine, oxybutynin, and the anticancer prodrugs capecitabine and CPT-11.[1–4] Consistent with their proposed function, CEs are expressed in high levels in human tissues such as the liver, lung, small intestine, and kidney. All CEs examined to date maintain a catalytic triad of amino acids (serine, histidine, and glutamic acid) that are essential for hydrolytic activity.

As CEs are responsible for the metabolism and activation of a host of different clinically useful agents, we have hypothesized that selective inhibitors of these enzymes may be useful in modulating the biological activity of these drugs. For example, for compounds that are inactivated by CEs (e.g., flestolol), addition of an inhibitor may prolong the period of time for which the drug is active.[5] Conversely for drugs that are activated by these enzymes (e.g., CPT-11), specific CE inhibitors may be useful in ameliorating the toxicity associated with these agents.[6] Therefore, we have screened for compounds that have selective inhibitory activity toward CEs. This was performed using Telik's Target Related Affinity Profiling (TRAP) technology.[7–9] Following the identification of compounds that demonstrated activity toward three mammalian CEs (human intestinal CE (hiCE), human liver CE (hCE1), and rabbit liver CE (rCE)), these chemicals were then assessed for their inhibition of human acetylcholinesterase (AChE). Molecules that inhibited the latter enzyme were discarded. This process identified benzil as a general, selective inhibitor of mammalian CEs.[10] More recent studies have shown that the characteristics for a good CE inhibitor are the presence of: (i) aromatic rings or increasing hydrophobicity, (ii) a 1,2-dione moiety, and (iii) substitution which does not impede access of the compound reaching the active site of the enzyme.[10,11] These studies also demonstrated that benzoin (2-hydroxy-1,2-diphenylethanone), an

Abbreviations: AChE, acetylcholinesterase; AcTCh, acetylthiocholine; BChE, butyrylcholinesterase; BuTCh, butyrylthiocholine; CE, carboxylesterase; CPT-11, irinotecan, 7-ethyl-10-[4-(1-piperidino)-1-piperidino]carbonyloxycamptothecin; EDG, electron donating group; EWG, electron withdrawing group; hCE1, human carboxylesterase 1; hiCE, human intestinal carboxylesterase; K_i, inhibition constant; *o*-NPA, *o*-nitrophenyl acetate; q^2, cross validation coefficient; QSAR, quantitative structure–activity relationship; rCE, rabbit liver carboxylesterase; TRAP, Target Related Affinity Profiling.

Keywords: Fluorobenzil; Fluorobenzoin; Carboxylesterase; Inhibitor.

* Corresponding author. Tel.: +1 901 495 3440; fax: +1 901 495 4293; e-mail: phil.potter@stjude.org

0968-0896/$ - see front matter © 2007 Elsevier Ltd. All rights reserved.
doi:10.1016/j.bmc.2007.03.012

intermediate in the synthesis of benzil from benzaldehyde, was a poor inhibitor of CEs, consistent with the hypothesis that the 1,2-dione chemotype is important in enzyme inhibition.

We believe that the benzils are potent inhibitors, in part, because the 1,2-dione structure mimics the ester chemotype allowing for the initiation of the nucleophilic addition-elimination reactions that are observed for this class of compounds (Fig. 1a). Abortive nucleophilic attack by the active site serine on one of the carbonyl carbons would yield a tetrahedral intermediate that would be unlikely to undergo C–C cleavage, the next step in the reaction. Therefore, in the presence of benzil, repetitive attack and release by the serine residue on the carbonyl groups would occur, resulting in enzyme inhibition. This hypothesis suggests that decreasing the electron density around the carbonyl carbon atom would make this atom more susceptible to nucleophilic attack by the serine oxygen. Therefore, appropriate inclusion of electron withdrawing groups (EWG) should increase the likelihood of attack and presumably the potency of the inhibitors (Fig. 1b). In this series of studies, we also assessed the ability of the benzoin to inhibit the mammalian CEs. Benzoins (α-hydroxy ketones) were chosen because they are key intermediates in the synthesis of benzils from the aldehydes and they possess similar structural characteristics to benzil, that is, aromatic rings, carbonyl groups, etc. (see Tables 1 and 2). While we have previously demonstrated that the benzoins are poor inhibitors of CEs,[10] modification of the electron density associated with the dione carbon atom, might have the potential to produce compounds that demonstrate inhibitory activity.

To test these hypotheses, we have synthesized a panel of fluorobenzoins and their analogous fluorobenzils, and assessed them for CE inhibition using hiCE, hCE1, and rCE. Results presented here indicate that fluorine substitution within the benzene rings generates benzoin analogs that are potent inhibitors of mammalian CEs.

2. Results

2.1. Analysis of carboxylesterase inhibition by fluorobenzils

In a previous paper, we hypothesized that nucleophilic attack at one of the carbonyl groups within the 1,2-dione moiety of benzil (**2**) by the catalytic serine was, in part, responsible for enzyme inhibition (Fig. 1a).[10] We therefore surmised that substituted benzene rings, which would withdraw electron density from these carbon atoms, might improve the potency of CE inhibition (Fig. 1b). To assess the validity of this hypothesis, we synthesized a panel of fluorobenzoins and fluorobenzils for use in enzyme inhibition studies. The structures of the compounds used for these assays are shown in Tables 1 and 2.

The ability of these compounds to inhibit hiCE, hCE1, rCE, human AChE, and human BChE was then determined and the K_i values for enzyme inhibition are reported in Tables 3 and 4. As indicated, the fluorobenzil analogs were all relatively good inhibitors of CEs with K_i values ranging from 3 nm to 2.8 μM. The most potent inhibitor was 1,2-bis(2,3-difluorophenyl)ethane-1,2-dione (**23**), yielding a K_i value of 3.3 nM with rCE. Interestingly, the inhibition constants were as high as 2.84 μM with 1,2-bis[2,4-bis(trifluoromethyl)phenyl]ethane-1,2-dione (**32**), with hiCE. In general, inhibitors that were potent for one enzyme demonstrated similar levels of activity toward the other

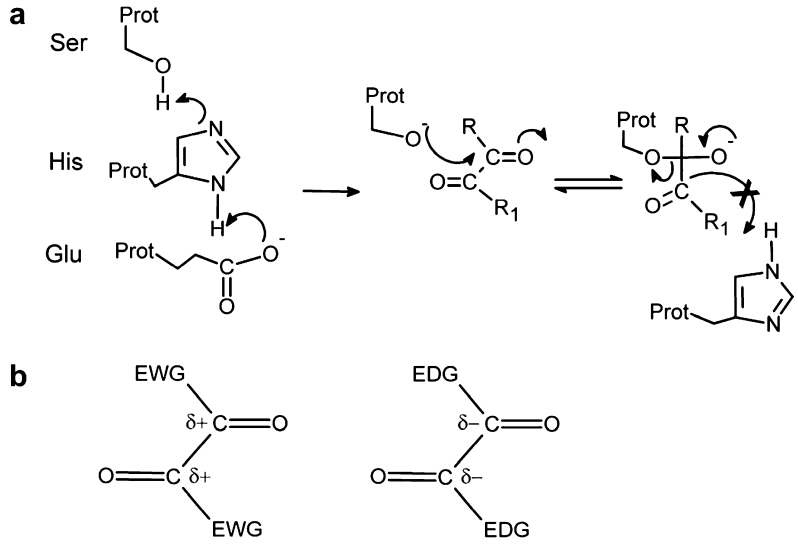

Figure 1. (a) Proposed mechanism of interaction of the benzil analogs with the catalytic amino acids of CEs. A serine nucleophile is generated by proton transfer to a glutamic acid via a histidine residue, and the resulting oxygen atom attacks one of the carbonyl groups within the dione moiety. The tetrahedral intermediate that is generated is relatively stable, due to the increased strength of the C–C bond as compared to the C–O bond present in esters. Therefore the former bond is not cleaved resulting in inhibition of the enzyme. (b) Increasing or decreasing the electron density surrounding the carbonyl carbon atoms by introducing either electron withdrawing groups (EWG) or electron donating groups (EDG) within the molecules should make the compounds better and poorer enzyme inhibitors, respectively.

Table 1. Structure of the fluorobenzoins used in this study

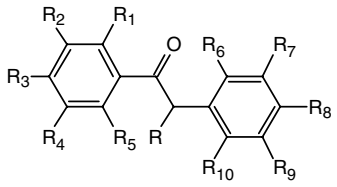

R = H unless otherwise indicated

ID	Name	R	R_1	R_2	R_3	R_4	R_5	R_6	R_7	R_8	R_9	R_{10}
1	Benzoin (1,2-diphenyl-2-hydroxy-ethanone)	OH										
3	1,2-Bis-(2-fluorophenyl)-2-hydroxyethanone	OH	F					F				
4	1,2-Bis-(3-fluorophenyl)-2-hydroxyethanone	OH		F					F			
5	1,2-Bis(4-fluorophenyl)-2-2-hydroxyethanone	OH			F					F		
6	1,2-Bis(2,4-difluorophenyl)-2-hydroxyethanone	OH	F		F			F		F		
7	1,2-Bis-(2,6-difluorophenyl)-2-hydroxyethanone	OH	F				F	F				F
8	1,2-Bis(3,4-difluorophenyl)-2-hydroxyethanone	OH		F	F				F	F		
9	1,2-Bis(2,3-difluorophenyl)-2-hydroxyethanone	OH	F	F				F	F			
10	1,2-Bis(2,5-difluorophenyl)-2-hydroxyethanone	OH	F			F		F			F	
11	1,2-Bis(3,5-difluorophenyl)-2-hydroxyethanone	OH		F		F			F		F	
12	1,2-Bis-(2,3,5-trifluorophenyl)-2-hydroxyethanone	OH	F	F		F		F	F		F	
13	1,2-Bis-(2,3,4-trifluorophenyl)-2-hydroxyethanone	OH	F	F	F			F	F	F		
14	1,2-Bis-(3,4,5-triflu0rophenyl)-2-hydroxyethanone	OH		F	F	F			F	F	F	
15	1,2-Bis-[4-(trifluoromethyl)phenyl]-2-hydroxyethanone	OH			CF_3					CF_3		
16	1,2-Bis-[3-(trifluoromethyl)phenyl]-2-hydroxyethanone	OH		CF_3					CF_3			

Table 2. Structure of the fluorobenzils used in this study

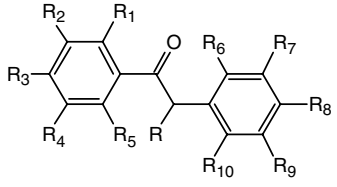

R = H unless otherwise indicated

ID	Name	R	R_1	R_2	R_3	R_4	R_5	R_6	R_7	R_8	R_9	R_{10}
2	Benzil (diphenylethane-1,2-dione)	=O										
17	1,2-Bis-(2-fluorophenyl)-ethane-1,2-dione	=O	F					F				
18	1,2-Bis-(3-fluorophenyl)-ethane-1,2-dione	=O		F					F			
19	1,2-Bis(4-fluorophenyl)-ethane-1,2-dione	=O			F					F		
20	1,2-Bis(2,4-difluorophenyl)-ethane-1,2-dione	=O	F		F			F		F		
21	1,2-Bis(2,6-difluorophenyl)-ethane-1,2-dione	=O	F				F	F				F
22	1,2-Bis(3,4-difluorophenyl)-ethane-1,2-dione	=O		F	F				F	F		
23	1,2-Bis(2,3-difluorophenyl)-ethane-1,2-dione	=O	F	F				F	F			
24	1,2-Bis(2,5-difluorophenyl)-ethane-1,2-dione	=O	F			F		F			F	
25	1,2-Bis(3,5-difluorophenyl)-ethane-1,2-dione	=O		F		F			F		F	
26	1,2-Bis(2,3,6-trifluorophenyl)-ethane-1,2-dione	=O	F	F			F	F	F			F
27	1,2-Bis(2,3,5-trifluorophenyl)-ethane-1,2-dione	=O	F	F		F		F	F		F	
28	1,2-Bis(2,3,4-trifluorophenyl)-ethane-1,2-dione	=O	F	F	F			F	F	F		
29	1,2-Bis(3,4,5-trifluorophenyl)-ethane-1,2-dione	=O		F	F	F			F	F	F	
30	1,2-Bis[4-(trifluoromethyl)phenyl]-ethane-1,2-dione	=O			CF_3					CF_3		
31	1,2-Bis[3(trifluoromethyl)phenyl]-ethane-1,2-dione	=O		CF_3					CF_3			
32	1,2-Bis[2,4-bis(trifluoromethyl)phenyl]-ethane-1,2-dione	=O	CF_3		CF_3			CF_3		CF_3		
33	1,2-Bis[3,5-bis(trifluoromethyl)phenyl]-ethane-1,2-dione	=O		CF_3		CF_3			CF_3		CF_3	
34	1,2-Bis[2,5-bis(trifluoromethyl)phenyl]-ethane-1,2-dione	=O	CF_3			CF_3		CF_3			CF_3	

two CEs. Overall, these results demonstrate that these fluorobenzils are good inhibitors; however, fluorine substitution did not dramatically increase the inhibitory potency of these compounds as compared to benzil. The latter compound demonstrates K_i values of 15.1, 45.1, and 103 nM for hiCE, hCE1, and rCE, respectively.

The trifluoromethyl analogs were less effective CE inhibitors than the fluorobenzils. For example, only the *para*-substituted compound (**30**) inhibited all three mammalian enzymes. Indeed, none of the other trifluoromethyl analogs that we analyzed inhibited hCE1 and compounds **32**–**34** also failed to inhibit rCE. We believe that this is likely due to steric constraints afforded by the

Table 3. K_i values for enzyme inhibition using the benzoin analogs. Values for CEs were determined using *o*-NPA as a substrate, and those for AChE and BChE using AcTCh or BuTCh as a substrate, respectively

ID	hiCE $K_i \pm$ SE (nM)	hCE1 $K_i \pm$ SE (nM)	rCE $K_i \pm$ SE (nM)	AChE K_i (nM)	BChE K_i (nM)
1	2670 ± 1010	7210 ± 2410	>100,000	>100,000	>100,000
3	250 ± 23	990 ± 100	91.4 ± 44.0	>100,000	>100,000
4	640 ± 80	3130 ± 470	660 ± 45	>100,000	>100,000
5	>100,000[a]	>100,000	>100,000	>100,000	>100,000
6	390 ± 44	480 ± 30	140 ± 18	>100,000	>100,000
7	120 ± 9	190 ± 5	61.8 ± 2.9	>100,000	>100,000
8	150 ± 17	1300 ± 210	220 ± 22	>100,000	>100,000
9	260 ± 15	730 ± 60	200 ± 39	>100,000	>100,000
10	55.2 ± 3.7	230 ± 7	48.3 ± 1.7	>100,000	>100,000
11	71.0 ± 9.0	170 ± 16	18.4 ± 1.0	>100,000	>100,000
12	99.5 ± 9.2	665 ± 30	31.7 ± 3.9	>100,000	>100,000
13	25.7 ± 3.1	260 ± 13	8.3 ± 0.4	>100,000	>100,000
14	1040 ± 50	1000 ± 50	85.7 ± 4.6	>100,000	>100,000
15	400 ± 35	870 ± 390	12.9 ± 2.9	>100,000	>100,000
16	220 ± 17	>100,000	42.4 ± 4.4	>100,000	>100,000

[a] >100,000 indicates less than 50% enzyme inhibition at an inhibitor concentration of 100 μM, that is, essentially no inhibition.

CF_3 group(s), since we have previously demonstrated that the entrance to the active site of hCE1 is considerably smaller and less flexible than the other CEs.[12] As the trifluoromethyl compounds are more bulky than the other benzils assayed in these studies, it is likely that steric hindrance prevents access to hCE1 and rCE active sites, and hence they do not inhibit these proteins. The benzoin analogs of compounds **32**–**34** were not produced due to their direct oxidation to the benzil derivative under the reaction conditions employed. This is likely due to the electron-withdrawing effects of the trifluoromethyl groups resulting in increased reactivity of the oxygen atoms and hence facile oxidation to the corresponding benzil.

2.2. Analysis of carboxylesterase inhibition by fluorobenzoins

Benzoin, **1**, is not a good inhibitor of mammalian CEs; it demonstrates K_i values of 2.7 and 7.2 μM for hiCE and hCE1, respectively, and is inactive toward rCE.[10] However, the addition of fluorine atoms to the benzene rings in the benzoins resulted in compounds that were very potent inhibitors of CEs (Table 4). The majority of the fluorobenzoin analogs had K_i values ranging from 8 nM to 1.3 μM, with the most potent inhibitor being 1,2-bis(2,3,4-trifluorophenyl)-2-hydroxyethanone (**13**), yielding a K_i value of 8.3 nM with rCE. With some exceptions, the fluorobenzoins were more potent inhibitors than benzoin. In contrast to the benzil analogs, fluorine substitutions on the benzene rings resulted in marked increases in the inhibitory potency of the benzoins.

For example, compound **11** demonstrated K_i values of 71.1, 170, and 18.4 nM for hiCE, hCE1, and rCE, respectively. These values are 37- to 5400-fold lower than that observed for the unsubstituted benzoin (**1**) for the same enzymes. However, there were examples where the patterns of enzyme inhibition were very different. As an example, compounds **3** and **4** inhibited all three enzymes, but **5** did not inhibit any of the enzymes (see Table 3). The only difference between these analogs is the position of the single fluorine atom in the benzene ring. Our results suggest, therefore, that bond polarization plays a major role in *mono*-substituted aromatic rings causing inductive effects to prevail when influencing the electron density associated with the α carbon atom. This inductive effect is likely responsible for the differential inhibition of the three mammalian CEs across the *mono*-substituted series.

In the disubstituted analogs, it was apparent that resonance effects could account for the differences in the inhibition constants for the mammalian CEs. For example compound **11** demonstrated lower K_i values than **6** or **9**, probably due to withdrawal of electrons from the dione moiety via the fluorine atoms at the 3- and 5-positions on the benzene ring. Due to the distances involved, this is unlikely to be mediated by inductive effects, but rather due to the stabilization of resonance structures where the π electrons are conjugated via the benzene rings. Substitution of fluorine atoms at the 3- and 5-positions will enhance the stability of the resonance structures, yielding a more electron deficient environment at the dione carbon atoms. This would make them more susceptible to attack by the serine nucleophile and therefore better CE inhibitors.

2.3. Assessment of electronic parameters for the fluorobenzils and fluorobenzoins

Having demonstrated that fluorine substitution increased the potency of the fluorobenzoin analogs, we decided to evaluate the electron distribution within these compounds using computational methods. Therefore, we calculated a variety of electronic parameters for the fluorobenzoins and fluorobenzils using density functional theory (Table 5). These included the atomic charges of the oxygen and carbon atoms within the dione (or the hydroxy-ethanone) group, the pK_a of the hydroxyl group of the benzoins, and Hammett substituent constants. The results were then analyzed and compared to the K_i values for each compound, with each mammalian CE.

Table 4. K_i values for enzyme inhibition using the benzil analogs

ID	hiCE K_i ± SE (nM)	hCE1 K_i ± SE (nM)	rCE K_i ± SE (nM)	AChE K_i (nM)	BChE K_i (nM)
2	15.1 ± 2.0	45.1 ± 3.4	103 ± 20	>100,000	>100,000
17	55.9 ± 3.4	185 ± 1	47.8 ± 1.4	>100,000	>100,000
18	25.9 ± 5.1	100 ± 27	36.2 ± 7.3	>100,000	>100,000
19	170 ± 12	230 ± 11.8	400 ± 59	>100,000	>100,000
20	270 ± 41	370 ± 109	98.0 ± 28.8	>100,000	>100,000
21	830 ± 63	5650 ± 420	1170 ± 90	>100,000	>100,000
22	150 ± 17	300 ± 8	49.3 ± 6.3	>100,000	>100,000
23	4.98 ± 0.16	34.7 ± 2.7	3.34 ± 0.02	>100,000	1270 ± 100
24	61.4 ± 2.7	260 ± 24	60.8 ± 9.0	>100,000	>100,000
25	30.6 ± 3.4	97.2 ± 8.5	22.8 ± 3.5	>100,000	>100,000
26	40.7 ± 3.8	320 ± 33	33.8 ± 8.2	>100,000	>100,000
27	31.9 ± 8.8	140 ± 28	28.9 ± 10.1	>100,000	>100,000
28	13.6 ± 3.4	91.3 ± 12.3	3.3 ± 0.6	>100,000	>100,000
29	360 ± 62	470 ± 113	67.9 ± 4.5	>100,000	>100,000
30	180 ± 91	170 ± 45	12.7 ± 6.0	>100,000	>100,000
31	250 ± 55	>100,000	150 ± 38	>100,000	>100,000
32	2840 ± 950	>100,000	>100,000	>100,000	>100,000
33	550 ± 170	>100,000	>100,000	>100,000	>100,000
34	2370 ± 630	>100,000	>100,000	>100,000	>100,000

Values for CEs were determined using *o*-NPA as a substrate, and those for AChE and BChE using AcTCh or BuTCh as a substrate, respectively.

As can be seen in Table 6, no correlations were observed between the charges present on the carbonyl carbon or oxygen atoms with the benzils and the observed K_i values for CE inhibition. In addition, poor Spearman *r* correlation coefficients were seen with the predicted charge on the hydroxyl oxygen atom in the benzoins, when

Table 5. Calculated electronic parameters for the compounds used in this study

ID	Charge[a] **C**–OH	Charge[a] **C**=O	Charge[a] C–**O**H	Charge[a] C=**O**	Benzoin **O**H pK_a	Hammett δ
1	0.019	0.411	−0.531	−0.444	7.909	0
2		0.342		−0.462		0
3	0.029	0.389	−0.531	−0.444	7.487	1.060
4	0.022	0.412	−0.539	−0.442	7.214	0.674
5	0.017	0.411	−0.539	−0.452	7.209	0.124
6	0.034	0.410	−0.545	−0.444	6.668	0.592
7	0.041	0.386	−0.534	−0.426	7.230	1.060
8	0.020	0.414	−0.539	−0.445	7.713	0.399
9	0.027	0.395	−0.529	−0.439	7.052	0.867
10	0.026	0.373	−0.544	−0.394	6.719	0.867
11	0.028	0.410	−0.538	−0.436	8.435	0.674
12	0.025	0.401	−0.526	−0.433	6.855	1.204
13	0.034	0.412	−0.544	−0.438	7.079	0.929
14	0.022	0.418	−0.538	−0.439	8.342	0.736
15	0.029	0.347	−0.539	−0.452	10.764	1.080
16	0.021	0.418	−0.538	−0.440	10.784	0.860
17		0.317		−0.416		1.060
18		0.348		−0.456		0.674
19		0.343		−0.465		0.124
20		0.318		−0.419		0.867
21		0.337		−0.400		1.060
22		0.281		−0.376		0.399
23		0.321		−0.411		0.867
24		0.321		−0.410		0.867
25		0.353		−0.449		0.674
26		0.341		−0.395		1.397
27		0.326		−0.405		1.024
28		0.354		−0.445		0.929
29		0.352		−0.453		0.736
30		0.346		−0.452		1.080
31		0.349		−0.453		0.860
32		0.318		−0.414		0.750
33		0.357		−0.447		0.860
34		0.298		−0.400		0.640

[a] The charge on the respective atom is indicated in bold.

Table 6. Correlation coefficients for the atomic charges on the hydroxyl and the carbonyl oxygen and carbon atoms in the fluorobenzoins and the fluorobenzils, with the observed K_i values for CE inhibition

Compound	Atom[a]	Linear regression (r^2)			Spearman correlation coefficient (Spearman r)			p value for Spearman correlation[b]		
		hiCE	hCE1	rCE	hiCE	hCE1	rCE	hiCE	hCE1	rCE
Benzoins	**C**–OH	0.16	0.22	0.25	−0.470	−0.757	−0.533	0.077	**0.001**	**0.041**
	C=O	0.02	0.08	0.04	0.176	0.533	0.223	0.53	**0.04**	0.43
	C–**OH**	0.02	0.03	0.00	−0.198	−0.146	−0.013	0.48	0.60	0.96
	C=**O**	0.23	0.11	0.20	−0.672	−0.665	−0.518	**0.006**	**0.007**	**0.05**
Benzils	**C**=O	0.07	0.0	0.03	−0.118	−0.152	−0.166	0.63	0.53	0.50
	C=**O**	0.03	0.0	0.02	0.115	0.245	−0.041	0.64	0.31	0.87

[a] Charge on specific atom is indicated in bold.
[b] p values $\leqslant 0.05$ are indicated in bold.

Table 7. Correlation coefficients for the pK_a values for the hydroxyl proton in the fluorobenzoins with the observed K_i values for CE inhibition

Compound	Linear regression (r^2)			Spearman correlation coefficient (Spearman r)			p value for Spearman correlation		
	hiCE	hCE1	rCE	hiCE	hCE1	rCE	hiCE	hCE1	rCE
Benzoins	0.02	0.13	0.01	0.232	0.336	−0.170	0.41	0.22	0.55

Table 8. Correlation coefficients for the Hammett substituent constants for the fluorobenzoins and the fluorobenzils, with the observed K_i values for CE inhibition

Compound	Linear regression (r^2)			Spearman correlation coefficient (Spearman r)			p value for Spearman correlation[a]		
	hiCE	hCE1	rCE	hiCE	hCE1	rCE	hiCE	hCE1	rCE
Benzoins	0.26	0.11	0.63	−0.489	−0.462	−0.703	0.065	0.083	**0.004**
Benzils	0.0	0.0	0.0	−0.041	0.006	0.407	0.87	0.98	0.08

[a] p values $\leqslant 0.05$ are indicated in bold.

compared to the enzyme inhibition data. However, we observed significant p values (<0.05) for the correlation analyses when the charge on the carbonyl oxygen atom of the fluorobenzoins was compared to the K_i values for the mammalian CEs (Table 6). Additionally, a correlation ($p = 0.077$ with hiCE at the 10% level) was seen between the charge on the hydroxyl carbon atom and the K_i values for the inhibition of hCE1 and rCE with these compounds. Overall, these results indicate that the relative efficiency of inhibition by the benzoins is related to the electron density surrounding these atoms within the hydroxy-ethanone moiety. Perhaps not surprisingly, no obvious correlations were apparent when using linear regression analysis of the datasets (Table 6).

No correlations were seen between the K_i values for enzyme inhibition and the pK_a value of the hydroxyl proton in the benzoins (Table 7). Interestingly, a significant p value was seen for the correlation between the Hammett constants and the K_i values for rCE with the benzoins, but not, however, with the benzils (Table 8). This is likely a consequence of the lack of polarizability in the C–OH bond relative to the C=O bond.

2.4. QSAR analysis of fluorobenzoin- and fluorobenzil-mediated inhibition of carboxylesterases

Since the results obtained from the comparisons of the enzyme inhibition data and the electronic parameters indicated that the charge distribution within the central carbon atoms may be an important factor in CE inhibition, we performed 3D-QSAR analysis of the data using Quasar software. These experiments generated linear correlation coefficient (r^2) values ranging from 0.65 to 0.89 for the observed versus predicted K_i values for CE inhibition (Table 9; Fig. 2). In addition, excellent cross correlation coefficients (q^2) were obtained from these analyses. Since these values, and q^2/r^2 ratios, are all close to unity, these results suggest that the models have considerable predictive power in assessing CE inhibition by the benzoins and the benzils.

Graphic representations of the 3D-QSAR models for hCE1, hiCE, and rCE are depicted in Figure 3. No simple descriptor of the active site gorge would explain the inhibitory activity of the benzils and benzoins toward

Table 9. Correlation coefficients for the QSAR models

Compound	Enzyme	Observed versus predicted K_i values (r^2)	Cross correlation coefficient (q^2)	q^2/r^2
Benzoins	hiCE	0.816	0.751	0.92
	hCE1	0.914	0.861	0.94
	rCE	0.898	0.826	0.92
Benzils	hiCE	0.686	0.648	0.94
	hCE1	0.918	0.887	0.97
	rCE	0.885	0.848	0.96

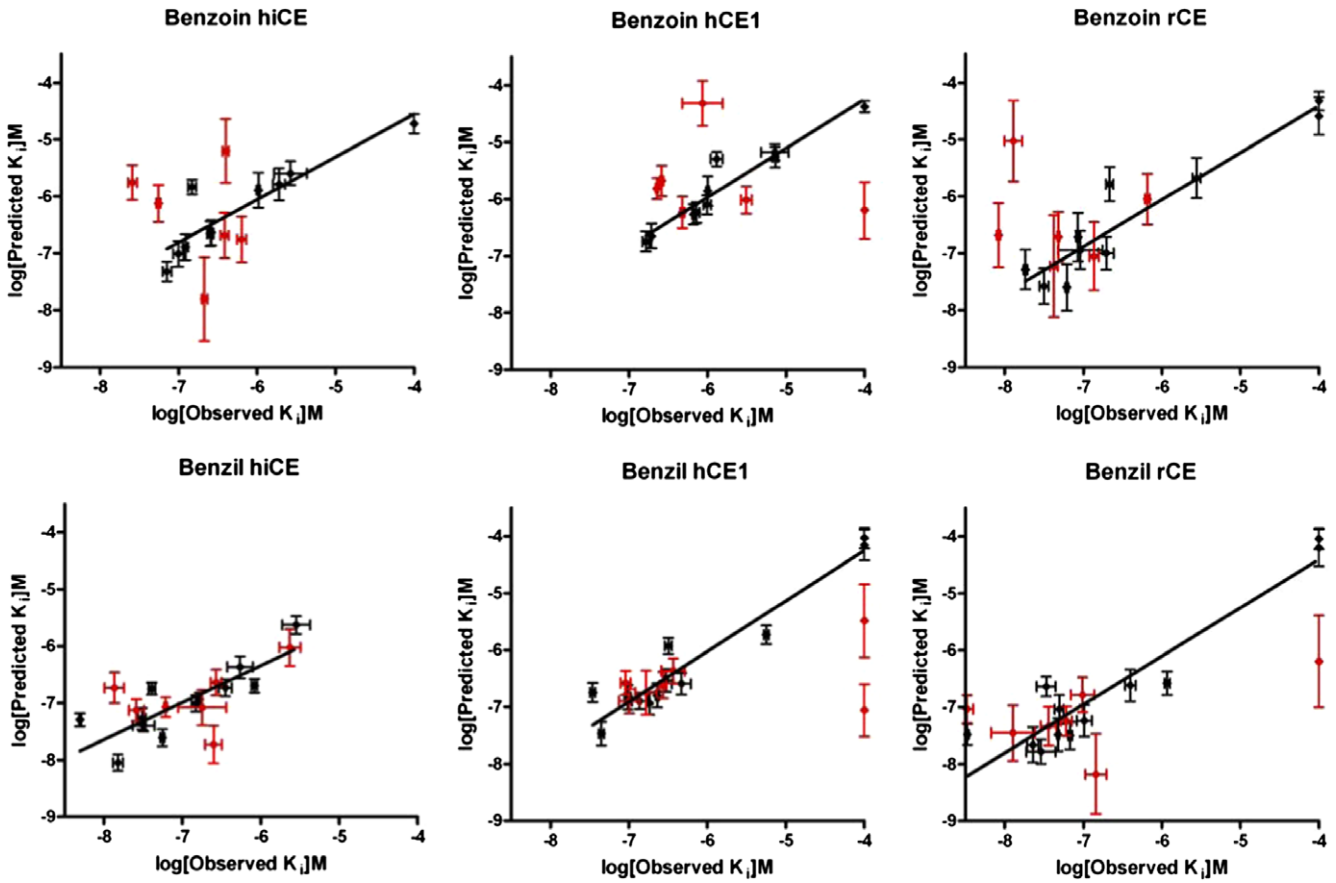

Figure 2. Graphs depicting the observed versus the predicted K_i values for the inhibition of the CEs following QSAR analysis. Data points used to construct the model are shown in black, and the test values are indicted in red.

each enzyme. Rather, as we previously observed with other benzil analogs,[10] it is the overall hydrophobic and electrostatic milieu of the binding site that contributes to the affinity of each analog, and these characteristics are slightly different for each enzyme.

3. Discussion

In this paper, we have examined the fluorine substituent effects on the inhibitory potency of a panel of fluorobenzoins and fluorobenzils toward mammalian CEs. These studies were initiated since we had previously hypothesized that the electron density surrounding the carbonyl carbon atoms in the 1,2-dione moiety may be an important factor in inhibitor potency.[10] If nucleophilic attack on these atoms, by the catalytic serine in the active site of the CE, is necessary for enzyme inhibition (Fig. 1), then reducing the electron density around the carbonyl carbons may make the inhibitors more potent. We reasoned that this could be achieved by introducing EWG (e.g., fluorine atoms) as substituents to the benzene rings of these compounds.

While inclusion of fluorine (or multiple fluorine atoms) within the benzil analogs did not dramatically improve their inhibitory potency, the corresponding benzoin compounds were considerably more potent CE inhibitors (Table 4). This effect was most pronounced when the fluorine atoms were either at the *ortho*- or the *meta*-positions. For example, compounds **3** (*ortho*-substituted) and **4** (*meta*-substituted) demonstrated inhibition toward all CEs, whereas **5** (*para*-substituted) displayed no inhibitory effect toward any of the enzymes (see Table 4). The lack of increase in the potency of the fluorobenzil analogs may be due to the fact that the electrons in both the σ and the π orbitals in the carbonyl bonds are principally distributed toward the more electronegative O atom. Therefore, any attempt to reduce the electron density surrounding the carbon atom (by substituting EWG groups in the benzene ring) will actually redistribute the electrons within the polarizable π bond toward the carbon atom. This would reduce the overall positive charge on this atom (consistent with the results seen in Table 5) rendering it less susceptible to nucleophilic attack. This is also consistent with our experimental results (e.g., most of the fluorobenzils are poorer inhibitors of the human CEs than benzil; Table 4). The change in the electron density, due to polarization of the C–OH bond in the fluorobenzoins by addition of fluorine atoms, would be much less pronounced and hence this effect is unlikely to be observed with these compounds. Again, this is born out

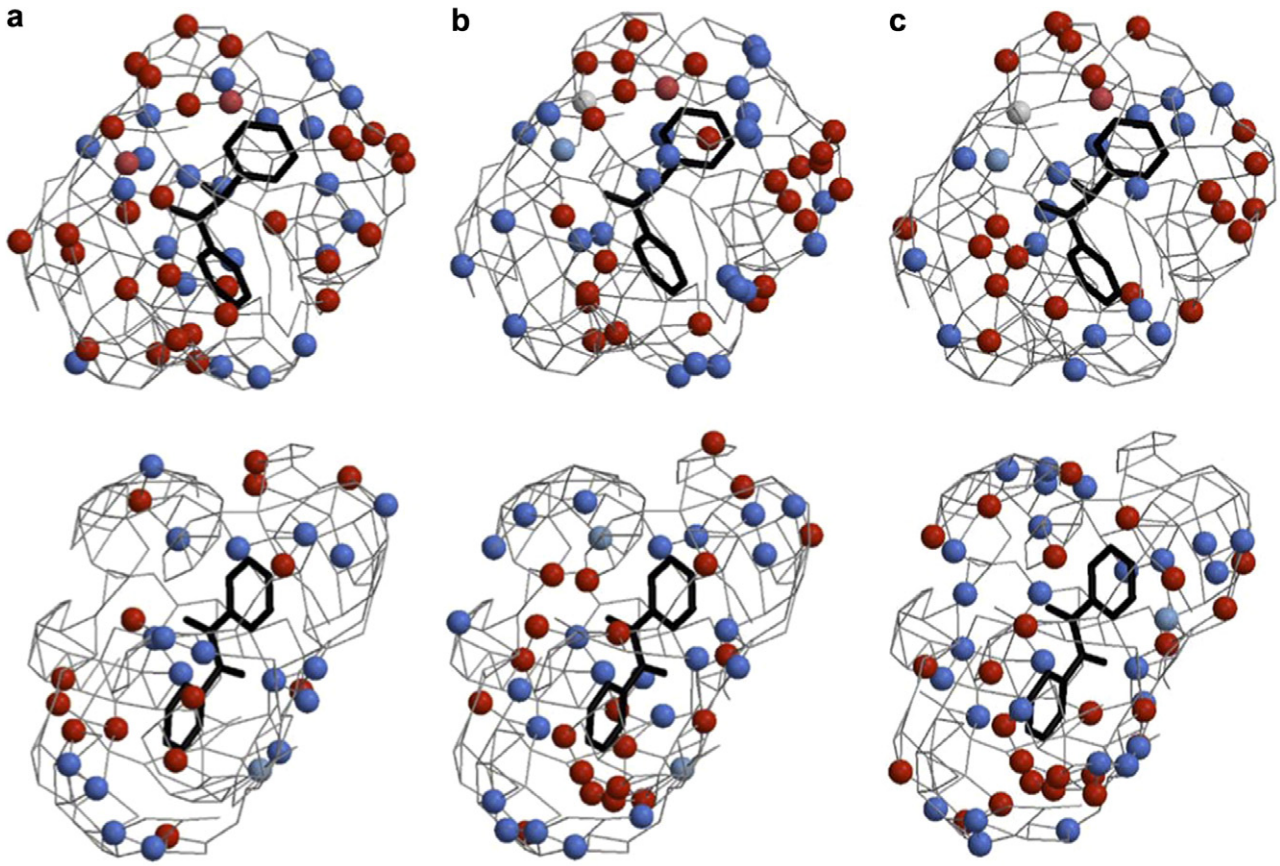

Figure 3. 3D-QSAR pseudoreceptor models for the inhibition of CEs by the fluorobenzoins (upper panel) and the fluorobenzils (lower panel). In each case, the models for hiCE (a), hCE1 (b), and rCE (c) are shown as colored spheres on a hydrophobic gray grid. Areas that are hydrophobic are indicated in gray, with blue spheres representing regions that are positively charged and hydrophobic (+0.1e), and light blue spheres corresponding to hydrogen bond donors. Orange spheres indicate hydrogen bond acceptors and orange-red spheres correspond to areas that are negatively charged and hydrophobic (−0.1e). The structure of benzil or benzoin is shown in black. The figure was created using Raster3D and Molscript.[32]

by both the MO calculations (Table 5) and the inhibition assays (Table 3).

The substituent effects exerted by the fluorine atoms could be achieved by any one (or a combination) of three different properties. These include resonance, inductive, and/or field effects. Being highly electronegative, it is likely that the inductive effects produced by these atoms would be sufficient to modulate the inhibitory activity of the benzoin analogs. The results we obtained are consistent with the inductive effects exerted by the fluorine atoms via the sigma bonds in the molecule. Hence, when the fluorine groups are closer to the hydroxy-ethanone moiety (e.g., in the *ortho*-position), they have a more pronounced effect on the charge on the carbon atoms, and hence the K_i values are lower. In compounds where the fluorine group is further from the hydroxy-ethanone chemotype (e.g., the *meta*- or *para*-substituted analogs), there is a considerable reduction in the potency of these molecules as CE inhibitors. As a consequence, an order for the K_i values for the single substituted fluorobenzoins was observed where *ortho*-< *meta*- < *para*-(**3** < **4** < **5**). Similarly, with the di-substituted analogs, the *ortho-meta*-substituted benzoin (**10**) was more potent at CE inhibition than the *ortho-para*-analog (**6**). Again, these data are all consistent with the reduced inductive effects that would be exerted by the fluorine atoms in the *para*-position as compared to those in the *meta*-position.

Additionally, intramolecular hydrogen bonding between fluorine in the *ortho*-position and the benzoin hydroxyl hydrogen atom may influence inhibitor potency. Such a bond would generate a relatively stable 6-membered ring that may minimize or impede rotation of the benzene ring in the benzoin. Such an interaction might be favorable, for example, if the inhibitor is locked in a conformation that is more potent at enzyme inhibition, or unfavorable, if the reverse is true. Comparison of the K_i values for different *ortho*-substituted benzoin analogs versus their *meta*-substituted isomers (e.g., **2** vs **3**, **6** vs **8** or **7** vs **11**) however, revealed no clear pattern of enzyme inhibition. This may be due to the fact that all of the biochemical assays are performed in aqueous solution (~55 M H_2O), and hence the formation of a stable F···H–O–C intramolecular hydrogen bond would be unlikely.

Attempts to correlate the predicted charge on the carbon atoms within the dione moiety of the benzils with the K_i values for CE inhibition proved unsuccessful (Table 6). However, similar analyses indicated that for the

benzoins, the charge on the hydroxyl carbon highly correlated with the inhibition constants. Indeed, Spearman r coefficients of −0.470, −0.757, and −0.533, and p values of 0.077, 0.001, and 0.041 were obtained for hiCE, hCE1, and rCE, respectively. Additionally, we observed similar correlation with the charges on the carbonyl oxygen atom and the K_i values (Table 6). This suggests that the initiating event in enzyme inhibition in the case of the benzoins is the interaction of the serine nucleophile with the hydroxyl carbon (Fig. 4a). Since the inhibition is reversible, the formation of any diol intermediate (Fig. 4a) is presumably transient and presumably repetitive removal and release of the proton on the hydroxyl carbon atom would occur. This mechanism would account for the inhibition of the CEs.

Alternatively, since the acidity and hence the lability of the hydroxyl proton is mediated in part by the electronegativity of the carbon atom, it is possible that the O^- present within the serine may remove this proton to regenerate the amino acid (Fig. 4b). Again, this would likely be in rapid equilibrium such that upon removal of the inhibitor, free active protein would be obtained. It is currently unknown whether either of the above mechanisms is correct, but both chemical and structural studies are underway to assess the validity of these scenarios.

Since we did not identify one single parameter that would reflect the biological activity of all of the benzoins and the benzils, we used 3D-QSAR analysis of the datasets, to derive suitable relationships that would correlate the chemical structures of the inhibitors with their biological potency. The advantage of the 3D approach is that multiple parameters can be simultaneously evaluated and hence models that more accurately represent

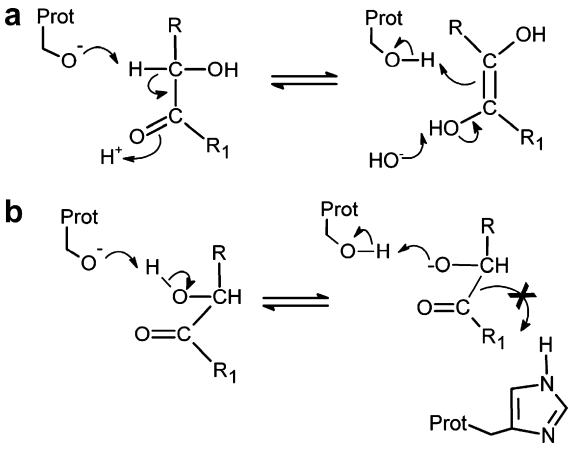

Figure 4. Proposed mechanism of inhibition of CEs by the fluorobenzoins. (a) The serine nucleophile (Prot-O^-) removes the proton on the hydroxy carbon atom to yield an intermediate that rearranges to form the ethylene diol analog. However, this species is probably in equilibrium with the benzoin and hence the reaction is readily reversible. This repetitive transfer of the proton likely inhibits the CE. (b) In a reversible process, the proton on the oxygen atom of the hydroxyl group of the benzoin is transferred to the serine oxygen atom. This results in the formation of the hydroxyl moiety on the serine residue. However, this would likely be attacked by the oxygen atom in the benzoin to reform the starting materials.

the inhibition of CEs can be obtained. In addition, we have previously performed similar analyses for a variety of different CE inhibitors, generating highly predictive 3D-pseudoreceptor site models for the different mammalian proteins.[6,10]

Analysis of the inhibition data for the benzoins and the benzils using Quasar software yielded good r^2 values for the observed versus predicted K_i values (Table 9; Fig. 2). In addition, cross correlation coefficients (q^2) ranging from 0.65 to 0.89 were obtained for the datasets. Since q^2 provides a measure of the predictive power of the model, and values greater than 0.4 are generally assumed to be suitable for use in biological systems,[13] our results suggest that the 3D-pseudoreceptor site models will be useful in the design of novel fluorine-based benzoin and benzil CE inhibitors.

Six inhibitors with known K_i values were used to test the ability of the benzoin models to predict K_i values, while seven were used to test the benzil models. In general, prediction was accurate (as indicated in Fig. 2). However, in all of the benzoin models, compound **15**, having symmetric *p*-trifluoromethyl groups on the phenyl rings, was systematically predicted to be a better inhibitor than was observed experimentally. Likewise, the inhibition constants for the benzil analog **31** were mis-predicted for hCE1 and rCE. Analysis of the models and data did not reveal any obvious reason why these inhibitors should have lower biological activity than was predicted. We hypothesize that these inhibitors may be interacting with sites on the surface of the CEs that cannot be accounted for in the K_i data, particularly the opening to the active site gorge.[12] We have demonstrated that the entrance to the CE active site can influence substrate turnover and hence it is likely that the same holds true for enzyme inhibitors.

For example, **31** was correctly predicted by the QSAR model to have good inhibitory activity toward rCE. As rCE has a demonstrably larger opening to the entrance to the active site gorge on the surface of the enzyme, this presumably allows access of bulkier inhibitors to the catalytic amino acids. Since both hiCE and hCE1 have more constrained active site entrances,[12] potentially facile access of compound **31** to the catalytic amino acids would be impeded. This would not be predicted in the current models. In contrast, the biological activity of compound **30** was accurately predicted by the QSAR models. Since **30** and **31** are isomers, we believe that it is unlikely that the low experimental K_i values of **31** would be so significantly different from those obtained with analog **30** unless interactions outside the active site were responsible.

Consistent with out previous studies, none of the benzoins or the benzils demonstrated any inhibitory activity toward AChE or BChE, with the exception of compound **23**. This fluorobenzil demonstrated reasonably good inhibition of BChE. The exact reason for this is unclear, especially since this compound failed to inhibit AChE. Interestingly, we have seen inhibition of both of

the cholinesterases by some nitrogen-containing fused ring diones (Hyatt et al., manuscript in preparation). These results suggest that this heteroatom is important for interaction of such molecules with the active sites of these proteins. This is perhaps not surprising since the choline group that is hydrolyzed from the choline esters contains a quaternary nitrogen that interacts with negatively charged amino acid residues within the cholinesterase active sites. This so-called anionic site is critical for efficient hydrolysis of these esters. Since none of the phenylethane-1,2-diones, or their hydroxy-ethanone analogs that we have assayed, can form stable positively charged quaternary compounds, we believe it is unlikely that these inhibitors would demonstrate activity toward AChE or BChE. The data presented here, and in previous publications,[10,11] support this hypothesis.

Overall our studies suggest that the mechanism of CE inhibition by benzil and its analogs works via abortive nucleophilic attack of the active site serine toward one of the carbonyl groups within the molecule (Fig. 1). Substitution of fluorine within the benzene rings did not alter benzil potency, but resulted in a significant increase in the inhibitory activity of the corresponding benzoins. This is likely due to a decrease in the electron density surrounding the target carbon atom, resulting in more facile attack by the serine nucleophile. In summary, these studies should allow the design of more potent selective CE inhibitors.

4. Experimental

4.1. General

Thiamine, copper acetate, ammonium nitrate, and fluorobenzaldehydes were purchased from Sigma–Aldrich (St. Louis, MO). Product formation was monitored by thin layer chromatography TLC using pre-coated silica gel GF plates (Analtech Inc., Newark, DE) and visualized using UV light (254 nm). Melting points were determined using a Mel-temp (Barnstead International, Dubuque, IA) and are reported uncorrected. NMR spectra (^{1}H and ^{13}C) were obtained using a Bruker DPX-400 (400 MHz) spectrometer using $CDCl_3$ (Aldrich) as a solvent and chemical shifts are reported in δ units (ppm) using tetramethylsilane as an internal standard with coupling constants (J) indicated in Hertz (Hz). Elemental analyses were performed by either Atlantic Microlabs (Norcross, GA) or Galbraith Laboratories (Knoxville, TN). Mass spectra were recorded on a VG 70-VSE(B) instrument (UIUC, Urbana-Champagne, IL) using EI or CI techniques.

4.2. Synthesis of fluorobenzoins

Fluorinated benzoins (1,2-diphenyl-2-hydroxy-ethanones) were synthesized by condensation of the correspondingly substituted fluorobenzaldehyde (0.04 mol) in the presence of thiamine hydrochloride (0.002 mol) in ethanolic sodium hydroxide (0.005 mol).[14] Routinely reactions were run at 50 °C for 48 h and following cooling on ice, crude product was filtered and washed with ice cold 75% ethanol. Material was re-crystallized from ethanol, and purity and structures were assessed by melting point, TLC, NMR, and total elemental analyses. All physical data for the synthesized compounds are shown in Table 10.

4.2.1. 1,2-Bis(2-fluorophenyl)-2-hydroxyethanone (3). 1,2-Bis(2-fluorophenyl)-2-hydroxyethanone was synthesized from 2-fluorobenzaldehyde. Physical and NMR parameters of **3** were consistent with those found in the literature.[15]

4.2.2. 1,2-Bis(3-fluorophenyl)-2-hydroxyethanone (4). 1,2-Bis(3-fluorophenyl)-2-hydroxyethanone was synthesized by the condensation of 3-fluorobenzaldehyde. Physical and NMR parameters of **4** were consistent with those previously reported.[15]

4.2.3. 1,2-Bis(4-fluorophenyl)-2-hydroxyethanone (5). 1,2-Bis(4-fluorophenyl)-2-hydroxyethanone was synthesized from 4-fluorobenzaldehyde to give white crystals in 75% yield.

4.2.4. 1,2-Bis(2,4-difluorophenyl)-2-hydroxyethanone (6). 1,2-Bis(2,4-difluorophenyl)-2-hydroxyethanone was synthesized from 2,4-difluorobenzaldehyde to give white crystals in 67% yield.

4.2.5. 1,2-Bis(2,6-difluorophenyl)-2-hydroxyethanone (7). 1,2-Bis(2,6-difluorophenyl)-2-hydroxyethanone was synthesized from 2,6-difluorobenzaldehyde to give white crystals in 72% yield.

4.2.6. 1,2-Bis(3,4-difluorophenyl)-2-hydroxyethanone (8). 1,2-Bis(3,4-difluorophenyl)-2-hydroxyethanone was synthesized from 3,4-difluorobenzaldehyde to give white crystals in 70% yield.

4.2.7. 1,2-Bis(2,3-difluorophenyl)-2-hydroxyethanone (9). 1,2-Bis(2,3-difluorophenyl)-2-hydroxyethanone was synthesized from 2,3-difluorobenzaldehyde to give white crystals in 73% yield.

4.2.8. 1,2-Bis(2,5-difluorophenyl)-2-hydroxyethanone (10). 1,2-Bis(2,5-difluorophenyl)-2-hydroxyethanone was synthesized from 2,5-difluorobenzaldehyde to give white crystals in 72% yield.

4.2.9. 1,2-Bis(3,5-difluorophenyl)-2-hydroxyethanone (11). 1,2-Bis(3,5-difluorophenyl)-2-hydroxyethanone was synthesized from 3,5-difluorobenzaldehyde to give white crystals in 72% yield.

4.2.10. 1,2-Bis(2,3,5-trifluorophenyl)-2-hydroxyethanone (12). 1,2-Bis(2,3,5-trifluorophenyl)-2-hydroxyethanone was synthesized from 2,3,5-trifluorobenzaldehyde to give white crystals in 74% yield.

4.2.11. 1,2-Bis(2,3,4-trifluorophenyl)-2-hydroxyethanone (13). 1,2-Bis(2,3,4-trifluorophenyl)-2-hydroxyethanone was synthesized from 2,3,4-trifluorobenzaldehyde to give white crystals in 72% yield.

Table 10. Physical and NMR parameters for the compounds synthesized in this paper

ID	Mp	^{1}H NMR	^{13}C NMR	MS *m/z*	Elemental analysis
5	81–82	δ 7.95 (m, J = 7.9 Hz, 2H), δ 7.15 (m, J = 7.3 Hz, 2H), δ 7.0 (m, J = 7.0 Hz, 4H), δ 5.95 (s, 1H) δ 4.2 (bs, 1H)	δ 197.20 (C=O), δ 167.38 (Ar, C–F), δ 161.56 (Ar, C–F), δ 134.83 (Ar, C–C=O), δ 133.92 (Ar, C–C–OH), δ 131.70 (Ar, C–H), δ 129.26 (Ar, C–H), δ 116.37 (Ar, C–H), δ115.99 (Ar, C–H), δ 88.36 (C–OH)	248	Anal. ($C_{14}H_{10}F_2O_2$); Calcd (%): C, 67.74; H, 4.06; F, 15.31. Found (%): C, 67.81; H, 4.03; F, 15.44
6	83–85	δ 7.95 (m, J = 7.9 Hz, 1H), δ 7.75 (m, J = 7.5 Hz, 1H), δ 7.15 (m, J = 7.2 Hz, 2H), δ 7.05 (m, J = 7.0 Hz, 2H), δ 6.1 (s, 1H), δ 4.3 (bs, 1H)	δ 188.57 (C=O), δ 165.4 (Ar, C–F), δ 164.49 (Ar, C–F), δ 162.60 (Ar, C–F), δ 162.47 (Ar, C–F), δ 132.84 (Ar, C–H), δ 132.12 (Ar, C–H), δ 118.01 (Ar, C–C–OH), δ 117.90 (Ar, C–C=O), δ 112.69 (Ar, C–H), δ 111.99 (Ar, C–H), δ 111.68 (Ar, C–H), δ 105.15 (Ar, C–H), δ 78.62 (C–OH)	284	Anal. ($C_{14}H_8F_4O_2$); Calcd (%): C, 59.16; H, 2.84; F, 26.74. Found (%): C, 59.22; H, 2.73; F, 26.78
7	71–73	δ 7.51(m, J = 7.6 Hz, 1H),7.30 (m, J = 7.4 Hz, 1H), δ 7.20 (m, J = 7.2 Hz, 2H), δ 7.10 (m, J = 7.1 Hz, 2H), δ 6.01 (s, 1H) δ 4.2 (bs, 1H)	δ 197.2 (C=O), δ 162.70 (Ar, C–F), δ 159.26 (Ar, C–F), δ 133.86 (Ar, C–H), δ 130.13 (Ar, C–H), δ 115.23 (Ar, C–C=O), δ 112.54 (Ar, C–H), δ 112.17 (Ar, C–H), δ 110.12 (Ar, C–C–OH), δ 76.31 (C–OH)	284	Anal. ($C_{14}H_8F_4O_2$); Calcd (%): C, 59.16; H, 2.84; F, 26.74. Found (%): C, 59.23; H, 2.63; F, 26.75
8	62–64	δ 7.85 (m, J = 7.9 Hz, 4H), δ 7.41 (m, J = 7.4 Hz, 2H), δ 6.00 (s, 1H), δ 4.2 (bs, 1H)	δ 191.23 (C=O), δ 155.21 (Ar, C–F), δ 151.61 (Ar, C–F), δ 150.12 (Ar, C–F), δ 146.33 (Ar, C–F), δ 132.99 (Ar, C–C=O), δ 132.01 (Ar, C–C–OH), δ 127.54 (Ar, C–H), δ 126.92 (Ar, C–H), δ 124.12 (Ar, C–H), δ 121.36 (Ar, C–H), δ 119.62 (Ar, C–H), δ 117.35 (Ar, C–H), δ 82.41 (Ar, C–OH)	284	Anal. ($C_{14}H_8F_4O_2$); Calcd (%): C, 59.16; H, 2.84; F, 26.74. Found (%): C, 59.15; H, 2.66; F, 26.67
9	54–56	δ 7.60 (m, J = 7.6 Hz, 1H), δ 7.35 (m, J = 7.4 Hz, 1H), δ 7.10 (m, J = 7.1 Hz, 4H) δ 6.10 (s, 1H), δ 4.48 (bs, 1H)	δ 195.74 (C=O), δ 156.96 (Ar, C–F), δ 150.14 (Ar, C–F), δ 147.23 (Ar, C–F), δ 139.85 (Ar, C–F), δ 127.66 (Ar, C–C–OH), δ 127.25 (Ar, C–C=O), δ 125.36 (Ar, C–H), δ 125.33 (Ar, C–H), δ 124.93 (Ar, C–H), δ 122.7 (Ar, C–H), δ 120.52 (Ar, C–H), δ 117.96 (Ar, C–H), δ 78.65 (C–OH)	284	Anal. ($C_{14}H_8F_4O_2$); Calcd (%): C, 59.16; H, 2.84; F, 26.74. Found (%): C, 59.10; H, 2.80; F, 26.75

(*continued on next page*)

Table 10 (*continued*)

ID	Mp	^{1}H NMR	^{13}C NMR	MS *m*/*z*	Elemental analysis
10	91–93	δ 7.8 (m, J = 7.8 Hz, 2H) δ 7.50 (m, J = 7.5 Hz, 2H), δ 7.20 (m, J = 7.3 Hz, 2H), δ 6.2 (s, 1H), δ 4.55 (bs, 1H)	δ 188.44 (C═O), δ 159.91(Ar, C–F), δ 157.73 (Ar, C–F), δ 157.70 (Ar, C–F), δ 156.82 (Ar, C–F), δ 123.87 (Ar, C–C–OH), δ 123.62 (Ar, C–C═O), δ 122.09 (Ar, C–H), δ 118.38 (Ar, C–H), δ 118.25 (Ar, C–H), δ 117.93 (Ar, C–H), δ 116.39 (Ar, C–H), δ 115.37 (Ar, C–H), δ 79.26 (C–OH)	284	Anal. ($C_{14}H_8F_4O_2$); Calcd (%): C, 59.16; H, 2.84; F, 26.74. Found (%): C, 59.06; H, 2.70; F, 26.73
11	78–80	δ 7.25 (m, J = 7.4 Hz, 2H), δ 7.05 (m, J = 7.0 Hz, 1H), δ 6.95 (m, J = 6.9 Hz, 2H), δ 6.98 (m, 6.8 Hz, 1H), δ 5.95 (s, 1H), δ 4.15 (bs, 1H)	δ 192.3 (C═O), δ 164.50 (Ar, C–F), δ 161.3 (Ar, C–F), δ 139.23 (Ar, C–C═O), δ 138.86 (Ar, C–C–OH), δ 113.06 (Ar, C–H) δ 110.26 (Ar, C–H), δ 109.19 (Ar, C–H) δ 102.12 (Ar, C–H), δ 86.32 (C–OH)	284	Anal. ($C_{14}H_8F_4O_2$); Calcd (%): C, 59.16; H, 2.84; F, 26.74. Found (%): C, 59.18; H, 2.71; F, 26.6
12	73–75	δ 7.35 (d, J = 7.4 Hz, 1H), δ 7.15 (d, J = 7.2 Hz, 1H), δ 6.9 (d, J = 6.9 Hz, 1H), δ 6.65 (d, J = 6.7 Hz, 1H), δ 6.01 (s, 1H), δ 4.5 (bs, 1H)	δ 192.23 (C═O), δ 160.10 (Ar, C–F), δ 157.89 (Ar, C–F), δ 157.32 (Ar, C–F), δ 149.65 (Ar, C–F), δ 140.23 (Ar, C–F), δ 133.26 (Ar, C–F), 125.26 (Ar, C–C–OH), δ 124.45 (Ar, C–C═O), δ 113.66 (Ar, C–H), δ 112.19 (Ar, C–H), δ 110.87(Ar, C–H), δ 102.70 (Ar, C–H), δ 81.23 (C–OH)	320	Anal. ($C_{14}H_6F_6O_2$); Calcd (%): C, 52.52; H, 1.89; F, 35.60. Found (%): C, 52.56; H, 1.71; F, 35.43
13	63–65	δ 7.75 (m, J = 7.7 Hz, 1H), δ 7.50(m, J = 7.6 Hz, 1H), δ 7.35 (m, J = 7.3 Hz, 1H) δ 7.25 (m, J = 7.3 Hz, 1H) δ 6.0 (s, 1H), δ 4.50 (bs, 1H)	δ 191.23 (C═O), δ 157.32 (Ar, C–F), δ 151.56 (Ar, C–F), δ 148.0 (Ar, C–F), δ 143.65 (Ar, C–F), δ 140.95 (Ar, C–F), δ 139.99 (Ar, C–F), δ 130.26 (Ar, C–H), 129.26 (Ar, C–H), δ 123.45 (Ar, C–C–OH), δ 122.65 (Ar, C–C═O), δ 118.23 (Ar, C–H), δ 113.66 (Ar, C–H), δ 83.23 (C–OH)	320	Anal. ($C_{14}H_6F_6O_2$); Calcd (%): C, 52.52; H, 1.89; F, 35.60. Found (%): C, 52.45; H, 1.70; F, 35.51
14	75–77	δ 7.25 (s, 2H), δ 7.95 (s, 2H), δ 5.9 (s, 1H), δ 4.1 (bs, 1H)	δ 197.67(C═O), δ 161.34 (Ar, C–F), δ 152.36 (Ar, C–F), δ 145.27 (Ar, C–F), δ 140.28 (Ar, C–F), δ 133.96 (Ar, C–C═O), δ 133.72 (Ar, C–C–OH), δ 115.09 (Ar, C–H), δ 113.36 (Ar, C–H), δ 85.62 (C–OH)	348	Anal. ($C_{14}H_6F_6O_2$); Calcd (%): C, 52.52; H, 1.89; F, 35.60. Found (%): C, 52.44; H, 1.71; F, 35.51

15	87–89	δ 8.0 (d, J = 8.0 Hz, 2H), δ 7.85 (d, J = 7.7 Hz, 2H), δ 7.30 (d, J = 7.5 Hz, 2H), δ 7.2 (d, J = 7.3 Hz, 2H), δ 6.01 (s, 1H), δ 4.42 (bs, 1H)	δ 197.68 (C=O), δ 141.95 (Ar, C–C=O), δ 138.98 (Ar, C–C–OH), δ 135.61 (Ar, C–CF_3), δ 129.40 (Ar, C–CF_3), δ 128.10 (Ar, C–H), δ 126.84 (Ar, C–H), δ 125.94 (Ar, C–H), δ 124.12 (Ar, C–H), δ 123.69 (CF_3), δ 85.12 (C–OH)	348	Anal. ($C_{16}H_{10}F_6O_2$); Calcd (%): C, 55.18; H, 2.89; F, 32.73. Found (%): C, 55.20; H, 2.84; F, 33.00
16	56–58	δ 8.0 (s, 2H), δ 7.70 (d, J = 8.0 Hz, 2H), δ 7.60 (m, J = 7.9 Hz, 2H), δ 7.4 (d, J = 7.7 Hz, 2H), δ 6.01 (s, 1H), δ 4.42 (bs, 1H)	δ 191.32 (C=O), δ 136.89 (Ar, C–C=O), δ 136.55 (Ar, C–C–OH), δ 133.65 (Ar, C–H), δ 132.86 (Ar, C–H), δ 130.46 (Ar, C–CF_3), δ 129.55 (Ar, C–CF_3), δ 128.23 (Ar, C–H), δ 127. 56 (Ar, C–H), δ 126.71 (Ar, C–H), δ 125.91 (Ar, C–H), δ 124.0 (Ar, C–H), δ 123.99 (CF_3) δ 123.92 (CF_3), δ 85.18 (C–OH)	348	Anal. ($C_{16}H_{10}F_6O_2$); Calcd (%): C, 55.18; H, 2.89; F, 32.73. Found (%): C, 55.38; H, 2.85; F, 32.92
17	103–105	δ 8.05 (d, J = 8.0 Hz, 2H), δ 7.50 (m, J = 7.9 Hz, 2H), δ 7.05 (m, J = 7.7 Hz, 2H), δ 6.85 (m, J = 7.7 Hz, 2H)	δ 190.21 (C=O), δ 163.0 (Ar, C–F), δ 136.72 (Ar, C–H), δ 130.89 (Ar, C–H), δ 125.00 (Ar, C–H), δ 122.32 (Ar, C–C=O)	246	Anal. ($C_{14}H_8F_2O_2$); Calcd (%): C, 68.30; H, 3.28; F, 15.43. Found (%): C, 68.15; H, 3.18; F, 15.66
18	97–99	δ 7.74 (d, J = 8.0 HZ, 2H), δ 7.71 (d, J = 7.8 Hz, 2H), δ 7.51 (m, J = 7.5 Hz, 2H) δ 7.39 (d, J = 7.4 Hz, 2H)	δ 192.20 (C=O), δ 162.89 (Ar, C–F), δ 138.68 (Ar, C–C=O), δ 130.89 (Ar, C–H), δ 126.05 (Ar, C–H), δ 122.26 (Ar, C–H), δ 116.21 (Ar, C–H)	246	Anal. ($C_{14}H_8F_2O_2$); Calcd (%): C, 68.30; H, 3.28; F, 15.43. Found (%): C, 68.17; H, 3.25; F, 15.59
19	118–119	δ 8.05 (m, J = 7.9 Hz, 4H), δ 7.50 (m, J = 7.5 Hz, 4H)	δ 192.23 (C=O), δ 168.17 (Ar, C–F), δ 132.82 (Ar, C–H), δ 128.36 (Ar, C–C=O), δ 116.47 (Ar, C–H)	246	Anal. ($C_{14}H_8F_2O_2$); Calcd (%): C, 68.30; H, 3.28; F, 15.43. Found (%): C, 68.51; H, 3.20; F, 15.7
20	91–93	δ 8.49 (d, J = 8.0 Hz, 2H), δ 7.40 (m, J = 7.7 Hz, 2H), δ 7.20 (m, J = 7.8 Hz, 2H)	δ 188.45 (C=O), δ 169.48 (Ar, C–F), δ 165.32 (Ar, C–F), δ 134.38 (Ar, C–H), δ 118.38 (Ar, C–C=O), δ 115.71 (Ar, C–H), δ 110.67 (Ar, C–H)	282	Anal. ($C_{14}H_6F_4O_2$); Calcd (%): C, 59.59; H, 2.14; F, 26.93. Found (%): C, 59.32; H, 2.05; F, 26.77
21	163–165	δ 7.95 (m, J = 7.9 Hz, 2H), δ 7.45 (m, J = 7.4 Hz, 4H)	δ 185.07 (C=O), δ 162.37 (Ar, C–F), δ 135.86 (Ar, C–H), δ 112.39 (Ar, C–H), δ 111.84 (Ar, C–C=O)	282	Anal. ($C_{14}H_6F_4O_2$); Calcd (%): C, 59.59; H, 2.14; F, 26.93. Found (%): C, 59.59; H, 2.05; F, 27.13
22	107–109	δ 8.05 (d, J = 8.1 Hz, 2H), δ 7.85 (d, J = 7.9 Hz, 2H), δ 7.70 (m, J = 7.7 Hz, 2H)	δ 190.20 (C=O), δ 156.30 (Ar, C–F), δ 150.37 (Ar, C–F), δ 133.70 (Ar, C–C=O), δ 127.70 (Ar, C–H), δ 126.30 (Ar, C–H), δ 118.50 (Ar, C–H)	282	Anal. ($C_{14}H_6F_4O_2$); Calcd (%): C, 59.59; H, 2.14; F, 26.93. Found (%): C, 59.32; H, 2.08; F, 26.63
23	91–93	δ 7.85 (d, J = 8.0 Hz, 2H), δ 7.45 (m, J = 7.5 Hz, 2H), δ 7.25 (m, J = 7.4 Hz, 2H)	δ 188.60 (C=O), δ 157.50 (Ar, C–F), δ 150.0 (Ar, C–F), δ 128.50 (Ar, C–H), δ 126.50 (Ar, C–H), δ 125.10 (Ar, C–C=O), δ 123.00 (Ar, C–H)	282	Anal. ($C_{14}H_6F_4O_2$); Calcd (%): C, 59.59; H, 2.14; F, 26.93. Found (%): C, 59.45; H, 2.03; F, 26.98

(*continued on next page*)

Table 10 (*continued*)

ID	Mp	^{1}H NMR	^{13}C NMR	MS *m/z*	Elemental analysis
24	110–112	δ 8.49 (d, J = 8.1 Hz, 2H) δ 7.38 (m, J = 7.8 Hz, 2H), δ 7.39 (m, J = 7.7 Hz, 2H)	δ 188.50 (C═O), δ 160.20 (Ar, C–F), δ 157.75 (Ar, C–F), δ 124.75 (Ar, C–C═O), δ 122.10 (Ar, C–H), δ 118.20 (Ar, C–H), δ 116.50 (Ar, C–H)	282	Anal. ($C_{14}H_6F_4O_2$); calc. (%): C, 59.59; H, 2.14; F, 26.93. Found (%): C, 59.42; H, 2.08; F, 27.13
26	124-126	δ 7.45 (m, J = 7.4 Hz, 2H), δ 7.00 (m, J = 7.0 Hz, 2H)	δ 183.55 (C═O), δ 158.50 (Ar, C–F), δ 155.00 (Ar, C–F), δ 148.55 (Ar, C–F), δ 122.80 (Ar, C–H), δ 113.30 (Ar, C–CH), δ 112.0 (Ar, C–C═O)	318	Anal. ($C_{14}H_4F_6O_2$); Calcd (%): C, 52.85; H, 1.27; F, 35.83. Found (%): C, 52.62; H, 1.15; F, 35.49
27	98–100	δ 7.55 (m, J = 7.5 Hz, 2H), δ 7.30 (m, 2H)	δ 186.80 (C═O), δ 158.30 (Ar, C–F), δ 157.75 (Ar, C–F), δ 146.70 (Ar, C–F), δ 123.0 (Ar, C–C═O), δ 111.70 (Ar, C–H), δ 110.50 (Ar, C–H)	318	Anal. ($C_{14}H_4F_6O_2$); Calcd (%): C, 52.85; H, 1.27; F, 35.83. Found (%): C, 52.68; H, 1.16; F, 35.72
28	94–96	δ 7.86 (m, J = 7.9 Hz, 2H), δ 7.23 (m, J = 7.2 Hz, 2H)	δ 194.38 (C═O), δ 157.32 (Ar, C–F), δ 151.32 (Ar, C–F), δ 138.39 (Ar, C–F), δ 127.29 (Ar, C–H), δ 121.25 (Ar, C–H), δ 120.42 (Ar, C–C═O)	318	Anal. ($C_{14}H_4F_6O_2$); Calcd (%): C, 52.85; H, 1.27; F, 35.83. Found (%): C, 52.72; H, 1.21; F, 36.03
30	134–136	δ 8.10 (d, J = 8.1 Hz, 4H), δ 7.78 (d, J = 7.8 Hz, 4H)	δ 191.90 (C═O), δ 136.40 (Ar, C–CF_3), δ 135.25 (Ar, C–C═O), δ 130.37 (Ar, C–H), δ 126.18 (Ar, C–H), δ 124.63 (CF_3)	346	Anal. ($C_{16}H_8F_6O_2$); Calcd (%): C, 55.50; H, 2.33; F, 32.92. Found (%): C, 55.28; H, 2.20; F, 33.2
31	101–103	δ 8.30 (s, 2H), δ 8.18 (d, J = 8.2 Hz, 2H), δ 7.95 (d, J = 7.9 Hz, 2H), δ 7.78 (m, J = 7.7 Hz, 2H)	δ 191.32 (C═O), δ 139.05 (Ar, C–C═O), δ 132.14 (Ar, C–CF_3), δ 131.58 (Ar, C–H), δ 130.25 (Ar, C–H), δ 129.85 (Ar, C–H), δ 127.69 (Ar, C–H), δ 124.70 (CF_3)	346	Anal. ($C_{16}H_8F_6O_2$); Calcd (%): C, 55.50; H, 2.33; F, 32.92. Found (%): C, 55.31; H, 2.23; F, 33.21
32	103–105	δ 8.10 (s, 2H), δ 8.0 (d, J = 8.0 Hz, 2H), δ 7.78 (d, J = 7.7 Hz, 2H)	δ 188.45 (C═O), δ 136.68 (Ar, C–CF_3), δ 133.70 (Ar, C–C═O), δ 130.58 (Ar, C–H), δ 129.57 (Ar, C–CF_3), δ 128.79 (Ar, C–H), δ 124.29 (Ar, C–H), δ 123.78 (Ar, CF_3), δ 121.43 (Ar, CF_3)	483 $(M+H)^{+1}$	Anal. ($C_{18}H_6F_{12}O_2$); Calcd (%): C, 44.83; H, 1.25; F, 47.28. Found (%): C, 44.76; H, 1.18; F, 47.55
33	130–132	δ 8.00 (s, 4H), δ 7.80 (s, 2H)	δ 188.11 (C═O), δ 135.23 (Ar, C–C═O), δ 132.42 (Ar, C–CF_3), δ 129.03 (Ar, C–H), δ 128.10 (Ar, C–H), δ 124.11 (CF_3)	483 $(M+H)^{+1}$	Anal. ($C_{18}H_6F_{12}O_2$); Calcd (%): C, 44.83; H, 1.25; F, 47.28. Found (%): C, 44.83; H, 1.14; F, 47.47
34	135–137	δ 8.08 (s, 2H), δ 7.71 (d, J = 8.0Hz, 2H), δ 7.79 (d, J = 7.7Hz, 2H)	δ 188.09 (C═O), δ 134.38 (Ar, C–CF_3), δ 132.41 (Ar, C–CF_3), δ 131.33 (Ar, C–H), δ 130.01 (Ar, C–C═O), δ 127.31(Ar, C–H), δ 126.58 (Ar, C–H), δ 124.17(CF_3), δ 120.36 (CF_3)	483 $(M+H)^{+1}$	Anal. ($C_{18}H_6F_{12}O_2$); Calcd (%): C, 44.83; H, 1.25; F, 47.28. Found (%): C, 44.86; H, 1.09; F, 47.35

4.2.12. 1,2-Bis(3,4,5-trifluorophenyl)-2-hydroxyethanone (14). 1,2-bis(3,4,5-trifluorophenyl)-2-hydroxyethanone was synthesized from 3,4,5-trifluorobenzaldehyde to give white crystals in 70% yield.

4.2.13. 1,2-Bis[4-(trifluoromethyl)phenyl]-2-hydroxyethanone (15). 1,2-Bis[4-(trifluoromethyl)phenyl]-2-hydroxyethanone was synthesized from 4-trifluoromethylbenzaldehyde to give white crystals in 68% yield.

4.2.14. 1,2-Bis[3-(trifluoromethyl)phenyl]-2-hydroxyethanone (16). 1,2-Bis[3-(trifluoromethyl)phenyl]-2-hydroxyethanone was synthesized from 3-trifluoromethylbenzaldehyde to give white crystals in 69% yield.

4.3. Synthesis of fluorobenzils

The substituted fluorobenzils were synthesized by oxidation of the corresponding benzoin using copper acetate (0.001 mol) and ammonium nitrate (0.006 mol) in 80% acetic acid.[16] Briefly, the benzoin was refluxed for 90 min and following cooling, the product appeared as a solid yellow mass. After washing extensively with water and cold 75% ethanol, the benzil was re-crystallized from ethanol. Product purity was assessed as described above for the benzoins.

4.3.1. 1,2-Bis(2-fluorophenyl)ethane-1,2-dione (17). 1,2-Bis(2-fluorophenyl)ethane-1,2-dione was synthesized from **3** to give yellow crystals in 95% yield.

4.3.2. 1,2-Bis(3-fluorophenyl)ethane-1,2-dione (18). 1,2-Bis(3-fluorophenyl)ethane-1,2-dione was synthesized from **4** to give yellow crystals in 98% yield.

4.3.3. 1,2-Bis(4-fluorophenyl)ethane-1,2-dione (19). 1,2-Bis(4-fluorophenyl)ethane-1,2-dione was synthesized from **5** to give yellow crystals in 98% yield.

4.3.4. 1,2-Bis(2,4-difluorophenyl)ethane-1,2-dione (20). 1,2-Bis(2,4-difluorophenyl)ethane-1,2-dione was synthesized from **6** to give yellow crystals in 95% yield.

4.3.5. 1,2-Bis(2,6-difluorophenyl)ethane-1,2-dione (21). 1,2-Bis(2,6-difluorophenyl)ethane-1,2-dione was synthesized from **7** to give yellow crystals in 98% yield.

4.3.6. 1,2-Bis(3,4-difluorophenyl)ethane-1,2-dione (22). 1,2-Bis(3,4-difluorophenyl)ethane-1,2-dione was synthesized from **8** to give yellow crystals in 98% yield.

4.3.7. 1,2-Bis(2,3-fluorophenyl)ethane-1,2-dione (23). 1,2-Bis(2,3-fluorophenyl)ethane-1,2-dione was synthesized from **9** to give yellow crystals in 93% yield.

4.3.8. 1,2-Bis(2,5-difluorophenyl)ethane-1,2-dione (24). 1,2-Bis(2,5-difluorophenyl)ethane-1,2-dione was synthesized from **10** to give yellow crystals in 96% yield.

4.3.9. 1,2-Bis(3,5-difluorophenyl)ethane-1,2-dione (25). 1,2-Bis(3,5-difluorophenyl)ethane-1,2-dione was synthesized from **11** to give yellow crystals in 97% yield. Physical and NMR parameters of **25** were as previously described.[10]

4.3.10. 1,2-Bis(2,3,6-trifluorophenyl)ethane-1,2-dione (26). 1,2-Bis(2,3,6-trifluorophenyl)ethane-1,2-dione was synthesized from 2,3,6-trifluorobenzaldehyde under the conditions described for the benzoin reactions. This was presumably due to immediate oxidation of the benzoin to the corresponding benzil.

4.3.11. 1,2-Bis(2,3,5-trifluorophenyl)ethane-1,2-dione (27). 1,2-Bis(2,3,5-trifluorophenyl)ethane-1,2-dione was synthesized from **12** to give yellow crystals in 90% yield.

4.3.12. 1,2-Bis(2,3,4-trifluorophenyl)ethane-1,2-dione (28). 1,2-Bis(2,3,4-trifluorophenyl)ethane-1,2-dione was synthesized from the oxidation of **13** to give yellow crystals in 95% yield.

4.3.13. 1,2-Bis(3,4,5-trifluorophenyl)ethane-1,2-dione (29). 1,2-Bis(3,4,5-trifluorophenyl)ethane-1,2-dione was synthesized from **14** to give yellow crystals in 94% yield. Physical and NMR parameters of **29** were as previously described.[10]

4.3.14. 1,2-Bis[4-(trifluoromethyl)phenyl]ethane-1,2-dione (30). 1,2-Bis[4-(trifluoromethyl)phenyl]ethane-1,2-dione was synthesized from **15** to give yellow crystals in 97% yield.

4.3.15. 1,2-Bis[3-(trifluoromethyl)phenyl]ethane-1,2-dione (31). 1,2-Bis[3-(trifluoromethyl)phenyl]ethane-1,2-dione was synthesized from **16** to give yellow crystals in 90% yield.

4.4. Synthesis of 1,2-bis[2,4-bis(trifluoromethyl)phenyl]ethane-1,2-dione (32), 1,2-bis[3,5-bis(trifluoromethyl)phenyl]-ethane-1,2-dione (33), and 1,2-bis[2,5-bis(trifluoromethyl)-phenyl]ethane-1,2-dione (34)

Synthesis of the above compounds was achieved by direct condensation of the substituted benzaldehyde using the method described for the benzoins (see above). Under these conditions, the benzil analog was produced, presumably via immediate oxidation of the benzoin intermediate.

4.4.1. 1,2-Bis[2,4-bis(trifluoromethyl)phenyl]ethane-1,2-dione (32). 1,2-Bis[2,4-bis(trifluoromethyl)phenyl]ethane-1,2-dione was synthesized from bis-(2,4-trifluoromethyl)benzaldehyde to give yellow crystals in 76% yield.

4.4.2. 1,2-Bis[3,5-bis(trifluoromethyl)phenyl]ethane-1,2-dione (33). 1,2-Bis[3,5-bis(trifluoromethyl)phenyl]ethane-1,2-dione was synthesized from bis-(3,5-trifluoromethyl)benzaldehyde to give yellow crystals in 76% yield.

4.4.3. 1,2-Bis[2,5-bis(trifluoromethyl)phenyl]ethane-1,2-dione (34). 1,2-Bis[2,5-bis(trifluoromethyl)phenyl]ethane-1,2-dione was synthesized from bis-(2,5-trifluoromethyl)benzaldehyde to give yellow crystals in 76% yield.

4.5. Enzymes

Pure rCE and hCE1 were prepared as described previously.[17] hiCE was prepared by concentration of bacu-

lovirus media from Sf9 cells expressing a secreted form of the protein. While not homogeneous, the preparation was at least 60% pure. Since no CE activity is expressed or secreted from uninfected Sf9 cells, the only CE present in the culture media was the recombinant hiCE protein. The GenBank Accession Nos. of the cDNAs used to generate the enzymes for this study were as follows: hiCE, Y09616;[18] hCE1, M73499;[19] rCE, AF036930.[20]

Human acetylcholinesterase (AChE) and butyrylcholinesterase (BChE) were obtained from Sigma–Aldrich.

4.6. Inhibition of carboxylesterases

CE inhibition was assessed using a spectrophotometric multiwell plate assay using 3 mM *o*-nitrophenyl acetate (*o*-NPA) as a substrate.[6,11] Briefly, the test compound and substrate (*o*-NPA) were aliquoted into duplicate wells of a 96-well plate and enzyme was added using a multiwell pipettor. The rate of change in absorbance at 420 nm was measured at 15 s intervals for 5 min and compared to wells containing no inhibitor. Routinely, inhibitor concentrations ranged from 1 nM to 100 μM. All assays were performed in duplicate and included both positive (50 μM bis(4-nitrophenyl)phosphate) and negative controls (DMSO, no enzyme).

4.7. Inhibition of acetylcholinesterase and butyrylcholinesterase

The ability of compounds to inhibit AChE and BChE was performed as previously described using either 1 mM acetylthiocholine (AcTCh) or butyrylthiocholine (BuTCh), respectively, as substrates.[21,22]

4.8. Determination of K_i values

Data obtained from the above assays were fitted to the following equation[23] to determine the inhibition constant (K_i)

$$i = \frac{[\mathrm{I}]\{[\mathrm{s}](1-\hat{I}^2)+K_s(\hat{I}-\hat{I}^2)\}}{[\mathrm{I}]\{[\mathrm{s}]+\hat{I}\pm K_s\}+K_i\{\hat{I}\pm[\mathrm{s}]+\hat{I}\pm K_s\}}$$

where i is the fractional inhibition, [I] is the inhibitor concentration, [s] is the substrate concentration, α is the change in affinity of substrate for enzyme, β is the change in the rate of enzyme substrate complex decomposition, K_s is the dissociation constant for the enzyme substrate complex, and K_i is the inhibitor constant. Curve fits were generated (where α ranged from 0 to ∞ and β ranged from 0 to 1) using GraphPad Prism software (San Diego, CA) and those generating the highest r^2 values were further analyzed using Akaike's information criteria.[24,25] After determination of the best fit for the experimental data, K_i values were then calculated using Prism.

4.9. Computational chemistry

All calculations were carried out using the Gaussian 03 software package (Gaussian, Wallingford, CT). Each compound was constructed using Gauss-View and geometry optimizations were performed at the B3LYP/6-31G(p,d) level of theory.[26,27] Mulliken atomic charges for atoms within the molecules were calculated from these datasets. pK_a values were predicted using ChemSilico Predict v2.0 software (ChemSilico LLC, Tewksbury, MA) and Hammett substituent constants were obtained from previously published reports.[28]

4.10. Linear regression and Spearman correlation analyses

Datasets were analyzed using GraphPad Prism software. This allowed for simultaneous calculation of both linear regression correlates (r^2) and Spearman r coefficients. For the latter analyses, Spearman r values close to 1 or −1 indicate good correlations, whereas values closer to 0 indicate a lack of statistical correlation.

4.11. 3D-QSAR analysis

3D-QSAR analysis was performed as previously described.[6,10] Briefly, compounds were initially constructed using Chem3D and atom types were determined using the *antechamber* module of AMBER7 (University of California, San Francisco, CA). After assignment of partial atomic charges using the bond charge correction approach,[29] compounds were analyzed using Quasar 4.0 software.[29–31] This program generates a 3D-receptor-surface model that contains the molecular properties of both the receptor site and the ligand that will be docked into this domain. Typically, 200 independent models are generated for each dataset and these are evaluated to yield 7000 pseudoreceptor site models. Model evaluation was then performed until the cross correlation coefficients (q^2) exceed 0.7 for the observed versus the predicted K_i values. Routinely this produced correlation coefficients (r^2) of >0.9.

Acknowledgments

This work was supported in part by NIH Grants CA76202, CA79763, CA98468, CA108775, DA18116, a Cancer Center Core Grant P30 CA 21765, and by the American Lebanese Syrian Associated Charities.

References and notes

1. Cashman, J.; Perroti, B.; Berkman, C.; Lin, J. *Environ. Health Perspect.* **1996**, *104*, 23.
2. Khanna, R.; Morton, C. L.; Danks, M. K.; Potter, P. M. *Cancer Res.* **2000**, *60*, 4725.
3. Redinbo, M. R.; Bencharit, S.; Potter, P. M. *Biochem. Soc. Trans.* **2003**, *31*, 620.
4. Redinbo, M. R.; Potter, P. M. *Drug Discov. Today* **2005**, *10*, 313–325.
5. Molinoff, P. B.; Ruddon, R. W. In *Goodman s the Pharmacological Basis of Therapeutics*; Hardman, J. G., Limbird, L. E., Eds.; McGraw-Hill: New York, 1996; p 1905.
6. Wadkins, R. M.; Hyatt, J. L.; Yoon, K. J.; Morton, C. L.; Lee, R. E.; Damodaran, K.; Beroza, P.; Danks, M. K.; Potter, P. M. *Mol. Pharmacol.* **2004**, *65*, 1336.

7. Beroza, P.; Villar, H. O.; Wick, M. M.; Martin, G. R. *Drug Discov. Today* **2002**, *7*, 807.
8. Dixon, S. L.; Villar, H. O. *J. Chem. Inf. Comput. Sci.* **1998**, *38*, 1192.
9. Kauvar, L. M.; Higgins, D. L.; Villar, H. O.; Sportsman, J. R.; Engqvist-Goldstein, A.; Bukar, R.; Bauer, K. E.; Dilley, H.; Rocke, D. M. *Chem. Biol.* **1995**, *2*, 107.
10. Wadkins, R. M.; Hyatt, J. L.; Wei, X.; Yoon, K. J.; Wierdl, M.; Edwards, C. C.; Morton, C. L.; Obenauer, J. C.; Damodaran, K.; Beroza, P.; Danks, M. K.; Potter, P. M. *J. Med. Chem.* **2005**, *48*, 2905.
11. Hyatt, J. L.; Stacy, V.; Wadkins, R. M.; Yoon, K. J.; Wierdl, M.; Edwards, C. C.; Zeller, M.; Hunter, A. D.; Danks, M. K.; Crundwell, G.; Potter, P. M. *J. Med. Chem.* **2005**, *48*, 5543.
12. Wadkins, R. M.; Morton, C. L.; Weeks, J. K.; Oliver, L.; Wierdl, M.; Danks, M. K.; Potter, P. M. *Mol. Pharmacol.* **2001**, *60*, 355.
13. Lundstedt, T.; Seifert, E.; Abramo, L.; Thelin, B.; Nystrom, A.; Pettersen, J.; Bergman, B. *Chemometr. Intell. Lab. Syst.* **1998**, *42*, 3.
14. Mohrig, J. R.; Hammond, C. N.; Schatz, P. F.; Morrill, T. C. In *Modern Projects and Experiments in Organic Chemistry: Miniscale and Williamson Microscale*; W.H. Freeman & Co.: New York, 2003; pp 367–368.
15. Demir, A. S.; Sesenoglu, O.; Eren, E.; Hosrik, B.; Pohl, M.; Janzen, E.; Kolter, D.; Feldmann, R.; Dunkelmann, P.; Muller, M. *Adv. Synth. Catal.* **2002**, *344*, 96.
16. Weiss, M.; Appel, M. *J. Am. Chem. Soc.* **1948**, *70*, 3666.
17. Morton, C. L.; Potter, P. M. *Mol. Biotechnol.* **2000**, *16*, 193.
18. Schwer, H.; Langmann, T.; Daig, R.; Becker, A.; Aslanidis, C.; Schmitz, G. *Biochem. Biophys. Res. Commun.* **1997**, *233*, 117.
19. Munger, J. S.; Shi, G. P.; Mark, E. A.; Chin, D. T.; Gerard, C.; Chapman, H. A. *J. Biol. Chem.* **1991**, *266*, 18832.
20. Potter, P. M.; Pawlik, C. A.; Morton, C. L.; Naeve, C. W.; Danks, M. K. *Cancer Res.* **1998**, *52*, 2646.
21. Doctor, B. P.; Toker, L.; Roth, E.; Silman, I. *Anal. Biochem.* **1987**, *166*, 399.
22. Ellman, G. L.; Courtney, K. D.; Anders, V.; Featherstone, R. M. *Biochem. Pharmacol.* **1961**, *7*, 88.
23. Webb, J. L. In *Enzyme and Metabolic Inhibitors*. In *General Principles of Inhibition*; Academic Press Inc.: New York, 1963; Vol. 1.
24. Akaike, H. In *Information theory and an extension of the maximum likelihood principle*, Petrov, B. N.; Csaki, F., Eds.; Second International Symposium on Information Theory, Budapest, Akademiai Kiado: Budapest, 1973; pp 267–281.
25. Akaike, H. *IEEE Trans. Autom. Control* **1974**, *AC-19*, 716.
26. Stephens, P. J.; Devlin, F. J.; Chabalowski, C. F.; Frisch, M. J. *J. Phys. Chem.* **1994**, *98*, 11623.
27. Petersson, G. A.; Bennett, A.; Tensfeldt, T. G.; Al-Laham, M. A.; Shirley, W. A.; Mantzaris, J. *J. Chem. Phys.* **1988**, *89*, 2193.
28. Buckley, A.; Chapman, N. B.; Schorter, J. *J. Chem. Soc. B-Phys. Org.* **1969**, *2*, 195.
29. Jakalian, A.; Jack, D. B.; Bayly, C. I. *J. Med. Chem.* **2002**, *23*, 1623.
30. Vedani, A.; Dobler, M. *J. Med. Chem.* **2002**, *45*, 2139.
31. Vedani, A.; Dobler, M. *Quant. Struct.-Act. Relat.* **2002**, *21*, 382.
32. Kraulis, P. J. *J. Appl. Crystallogr.* **1991**, *24*, 946.